



Numerical modelling of circular plate anchors in sand under partially drained cyclic loading

R. Kurniadi*

The University of Melbourne, Melbourne, Australia

A. Roy, S.H. Chow, M.J. Cassidy

The University of Melbourne, Melbourne, Australia

*rkurniadi@student.unimelb.edu.au (corresponding author)

ABSTRACT: This study presents a numerical model of a horizontal circular plate anchor in dense sand under partially drained cyclic loading. The model employed the SANISAND-MS constitutive model and coupled stress-pore fluid diffusion analysis to capture the accumulated anchor displacement and excess pore pressure buildup during cyclic loading. The model parameters were calibrated to drained and undrained cyclic triaxial test results, revealing the necessity of two different parameter sets to appropriately capture the responses. The partially drained response of plate anchors was better matched using the drained cyclic parameters, with adjustment required in the MS parameter β . The model performance was validated by simulating three centrifuge tests with variations in cyclic mean load and amplitude. Some insights on the predictive capability and the limitations of the model are provided in this paper.

Keywords: Plate anchor; partially drained cyclic loading; SANISAND-MS; centrifuge test

1 INTRODUCTION

Offshore wind development is moving towards deeper waters, necessitating the use of floating wind turbines. Such turbines need ‘anchors’ for secured mooring. Considering plate anchors in offshore applications are typically large in dimension, the severe metocean loading at deeper waters can result in partially drained behaviour. Therefore, it is of interest to assess the cyclic responses of plate anchors under partially drained conditions for different cyclic load combinations.

The cyclic response of plate anchors in sand has been previously assessed through limited physical and numerical studies (e.g. Chow et al. 2020; Kurniadi et al. 2023). Numerical modelling can serve as a powerful tool for revealing the underlying mechanisms. The challenge in numerically modelling partially drained responses under cyclic loading lies primarily in the robustness of the constitutive model in capturing the strain accumulation and excess pore pressure generation under each loading cycle. In light of these uncertainties, this paper assesses the performance of an advanced constitutive model in capturing the cyclic behaviour in sands, namely SANISAND-MS (Liu et al. 2019).

The paper first discusses the challenges in calibrating the SANISAND-MS model at element level against a set of undrained cyclic triaxial tests,

extending from previously calibrated parameters for drained cyclic tests (Roy et al. 2024). Secondly, it evaluates the model's predictive capability on a boundary value problem involving a plate anchor under partially drained cyclic loading through a coupled stress-pore fluid diffusion analysis. Results show the model effectively captures liquefaction in loose sand, but struggles with cyclic mobility in dense sand. It also demonstrates potential in predicting accumulated displacement and excess pore pressure around plate anchors under partially drained cyclic loading, despite noted limitations.

2 MODEL DETAILS AND CALIBRATION

2.1 Details of SANISAND-MS model

The SANISAND-MS model was shown to be effective in capturing the ratcheting response of drained cyclic loading (Liu et al. 2019) and the excess pore pressure buildup in the pre-liquefaction phase of high-cyclic undrained loading (Liu et al. 2018). However, its performance under partially drained conditions remains unverified.

In order to use the model in partially drained conditions, it is reasonable to calibrate the model parameters associated with the memory surface (MS) formulation to both drained and undrained cyclic

triaxial tests. The model possesses three parameters linked to MS, i.e., μ_0 , ζ , and β . The parameter μ_0 influences the soil stiffness, such that progressive soil stiffening with loading cycles is captured by increasing the plastic modulus (K_p). At the current stress ratio (\mathbf{r}) and for a loading tensor \mathbf{n} , this is mathematically expressed as:

$$K_p = \frac{2}{3} p' \frac{b_0(\mathbf{r}_\theta^b - \mathbf{r}) \cdot \mathbf{n}}{(\mathbf{r} - \mathbf{r}_{in}) \cdot \mathbf{n}} \exp \left[\mu_0 \left(\frac{p'}{p_{atm}} \right)^{0.5} \left(\frac{b^M}{b_{ref}} \right)^2 \right] \quad (1)$$

with $b_0 (= G_0 h_0 (1 - c_h e) / \sqrt{(p' / p_{atm})})$ being a function of void ratio (e), stress level (p'), elastic shear modulus (G_0) and hardening parameter (h_0). The changes in soil fabric during cyclic loading are captured by varying MS size and position using:

$$dm^M = \sqrt{\frac{3}{2}} d\alpha^M : \mathbf{n} - \frac{m^M}{\zeta} f_{shr} \langle -d\varepsilon_{vol}^p \rangle \quad (2)$$

$$d\alpha^M = \frac{2}{3} \langle L^M \rangle h^M (\mathbf{r}_\theta^b - \mathbf{r}^M) \quad (3)$$

where m^M and α^M are the current MS size and centre of the MS locus respectively. The expansion in MS ($dm^M > 0$) is triggered by contractive deformations, which increase soil stiffness. In contrast, shrinkage in MS is allowed only during dilative deformations and controlled by model parameter ζ . Changes in dilatancy (D_ψ) due to changes in soil fabric under cyclic loading are accounted for by a dependence on the distance \tilde{b}_d^M as:

$$D_\psi = [A_0 \exp(\beta(\tilde{b}_d^M / b_{ref}))](\mathbf{r}_\theta^d - \mathbf{r}) : \mathbf{n} \quad (4)$$

where A_0 and β are model parameters, \tilde{b}_d^M the distance between the opposite projection of the current stress ratio on the memory and dilatancy surfaces along the $(-\mathbf{n})$ direction.

2.2 Calibration of MS model parameters

The numerical model (in Section 3) would be compared against centrifuge studies on plate anchors in UWA silica sand (properties in Table 1). Accordingly, the SANISAND-MS model parameters were calibrated to UWA silica sand for drained and undrained conditions. The MS parameter calibration for drained cyclic triaxial tests was detailed in Roy et al. (2024), while this study extends the calibration to undrained cyclic triaxial tests.

Three isotropically consolidated undrained cyclic triaxial tests were conducted using the UWA silica sand as summarised in Table 2. The triaxial samples

were prepared at a relative density (I_D) of 41 – 76% using wet pluviation.

Table 1. Physical properties of UWA silica sand

Soil Properties	UWA Silica sand*
Mean diameter, D_{50} (mm)	0.2
Coefficient of uniformity, U	1.68
Maximum void ratio, e_{max}	0.789
Minimum void ratio, e_{min}	0.512

* from Chow et al. (2020)

The samples were isotropically consolidated at initial mean effective stresses (p'_{in}) of 100 or 200 kPa to effectively capture a notable excess pore pressure buildup during cyclic loading. Undrained cyclic loading was then applied at 0.5 Hz with an amplitude ratio ($\varsigma = q^{ampl}/p'_{in}$, q^{ampl} being the cyclic deviatoric stress) of 0.2 or 0.3 to promote cyclic responses that would induce both contraction and dilation.

Table 2. Undrained cyclic triaxial test program

Test ID	I_D	p'_{in} (kPa)	q^{ampl} (kPa)	$\varsigma = q^{ampl}/p'_{in}$
TXU01	76	200	40	0.2
TXU02	74	200	60	0.3
TXU03	41	100	30	0.3

The triaxial results (Figure 1(c)) showed that liquefaction with flow-type failure occurred in loose sand (TXU03) at the number of cycle (N) of 12. For dense samples (TXU01 and TXU02), cyclic mobility was observed, characterised by butterfly-shaped loops at low p' (Figure 1(a) and (b)). Test TXU02, with a higher $\varsigma = 0.3$, reached cyclic mobility at $N = 215$, while test TXU01 at $\varsigma = 0.2$ reached cyclic mobility at $N = 3356$.

The measured responses at $N = 1$ were compared with simulations using the reported 16 drained parameters as shown in Figure 1(a-c). Insets in Figure 1(b) and (c) show that the simulation underpredicted contraction at $N = 1$ in tests TXU02 and TXU03 (red dotted lines) compared to the experiments. This can be improved by reducing the soil dilatancy parameter n^d from 3.4 to 2.5 (blue dotted lines). However, the drained parameters did not predict any liquefaction or cyclic mobilities (Figure 1(d-f)). Thus, recalibration was conducted against the undrained cyclic tests by varying the MS parameters (μ_0 , ζ , β) and using $n^d = 2.5$, while keeping the other parameters identical to the reported drained set as summarised in Table 3.

The MS parameter μ_0 was first recalibrated by fitting the excess pore pressure ratio ($R_u = \Delta u/p'_{in}$) against the number of cycles (N) before phase transformation (PT) in test TXU01 (Figure 1g), identified by a sharp increase in R_u . This was reasonably matched using $\mu_0 = 160$. As evident in

Figure 1(h), the MS shrinkage parameter ζ primarily controls the value at which R_u attains constancy, with $\zeta = 0.0001$ providing a good fit. Finally, the parameter β , which controls the post-dilation R_u paths (Figure 1i); was calibrated as $\beta = 6$, compromising slightly from the better match at $\beta = 10$ to fit all three cyclic tests.

Using the recalibrated parameters, the model can reasonably predict the initial liquefaction in dense sand (Figure 1d,e) and flow-type failure in loose sand (Figure 1f). These prediction of initial liquefaction ($R_u = 1$) for TXU01, TXU02 and TXU03 ($N = 2800, 250, 18$ in Figure 1(d-e) are in reasonable agreement with the experiments ($N = 3356, 215, 12$ in Figure 1(a-c)). Additionally, simulated responses using the drained parameter set ($n^d = 2.5$) up to the same initial liquefaction cycles ($N = 2800, 250$, and 18) are included in Figures 1(d-e) for comparison. These simulations exhibit a much stiffer response, showing no indication of liquefaction as discussed earlier.

Table 3. Calibrated parameters for UWA silica sand

Model parameters	Symbol	Drained (Roy et al., 2024)	Undrained
Elastic properties	G_0	135 (85*)	
	ν	0.14	
Critical state properties	Γ	0.812	
	λ	0.0189	
	ξ	0.7	
	M	1.296	Identical to drained
	c_1	0.7	
Yield surface	m	0.05	
Parameters influencing plastic modulus	h_{in}	7.5 (4.2*)	
	c_h	1.01	
	n^b	2.0	
Parameters influencing dilatancy	A_0	0.84	0.84
	n^d	3.4 (2.8*)	2.5
Memory surface (MS)	μ_0	85	160
	ζ	0.001	0.0001
	β	1.0 (2.0*)	6.0

*Final values adopted in modelling plate anchors

It is worth noting that experiments TXU01 and TXU02 also showed multiple butterfly-shaped loops at low mean stress, known as semifluidized state (Barrero et al. 2020), which the simulations failed to capture after initial liquefaction (Figure 1d, e). This known limitation (Barrero et al. 2020) prevents the model from effectively capturing large shear strains associated with a semifluidized state. Other versions, such as SANISAND-MSf has shown to overcome this limitation and could be explored to capture the cyclic mobility responses.

3 FINITE ELEMENT METHODOLOGY

To verify the performance of SANISAND-MS in simulating the partially drained cyclic response of a horizontal circular plate anchor in sand, an FE model was implemented in Abaqus using 4-node axisymmetric stress-displacement and pore-fluid elements (CAX4P). The plate was modelled as weightless and rigid, centred around the reference point (RP in

Figure 2). The plate, with a diameter (D) of 0.9 m and thickness (t) of 0.18 m, was wished in place at a depth (H) of 2.7 m ($H = 3D$) based on the scaled centrifuge model anchor (described later).

The soil domain was discretised with a total of 696 elements. The minimum mesh size around the anchor is $0.05D$, increasing to a maximum of $2D$ close to the domain boundary. The lateral boundary was set at $3H$ away from the axis of symmetry and the bottom boundary at $3D$ below the anchor base. Radial constraints were applied to the lateral boundary, whereas nodes in the bottom boundary were constrained in radial and vertical directions. Zero excess pore pressure boundary conditions were prescribed along the top boundary. The coefficient of lateral earth pressure at rest (K_0) was set as 0.5.

The FE model was developed for prototype-scaled anchors. To maintain the same degree of consolidation (dimensionless time factor, $T = c_v \cdot t / D^2$) between the prototype-scaled FE model and the corresponding centrifuge model, the time (t) in the FE model will need to be scaled by N_g^2 (N_g is the gravitational acceleration), which is not computationally efficient. Instead the coefficient of consolidation (c_v) or the permeability in the prototype (k_p) is scaled by a factor of N_g^2 to match the model scale (k_m), i.e. $k_p = N_g^2 k_m$. The permeability of methocel-saturated silica sand (k_m) was 3×10^{-4} m/s, but reduced by a factor equal to the dynamic viscosity ($\mu = 169$ mPas) of pore fluid methocel (reported later), resulting in a final $k_p = 0.0016$ m/s.

To model the interface tension developing beneath the anchor and possible gap formation during cyclic vertical loading, a thin layer of poroelastic gap elements (GE) having a thickness of $0.05D$ was kept beneath the anchor and ‘tied’ to the plate and the underlying soil (Maitra et al. 2019). The GE was kept 10^7 times more permeable than the soil with an elastic modulus of 0.01 kPa and Poisson’s ratio of 0.01.

The vertical cyclic stress was applied to the RP in two steps following a geostatic stress. Initially, the anchor was subjected to the mean stress. This was followed by applying the cyclic stress amplitude in

parallel with the mean stress within a ‘transient consolidation’ time step in Abaqus.

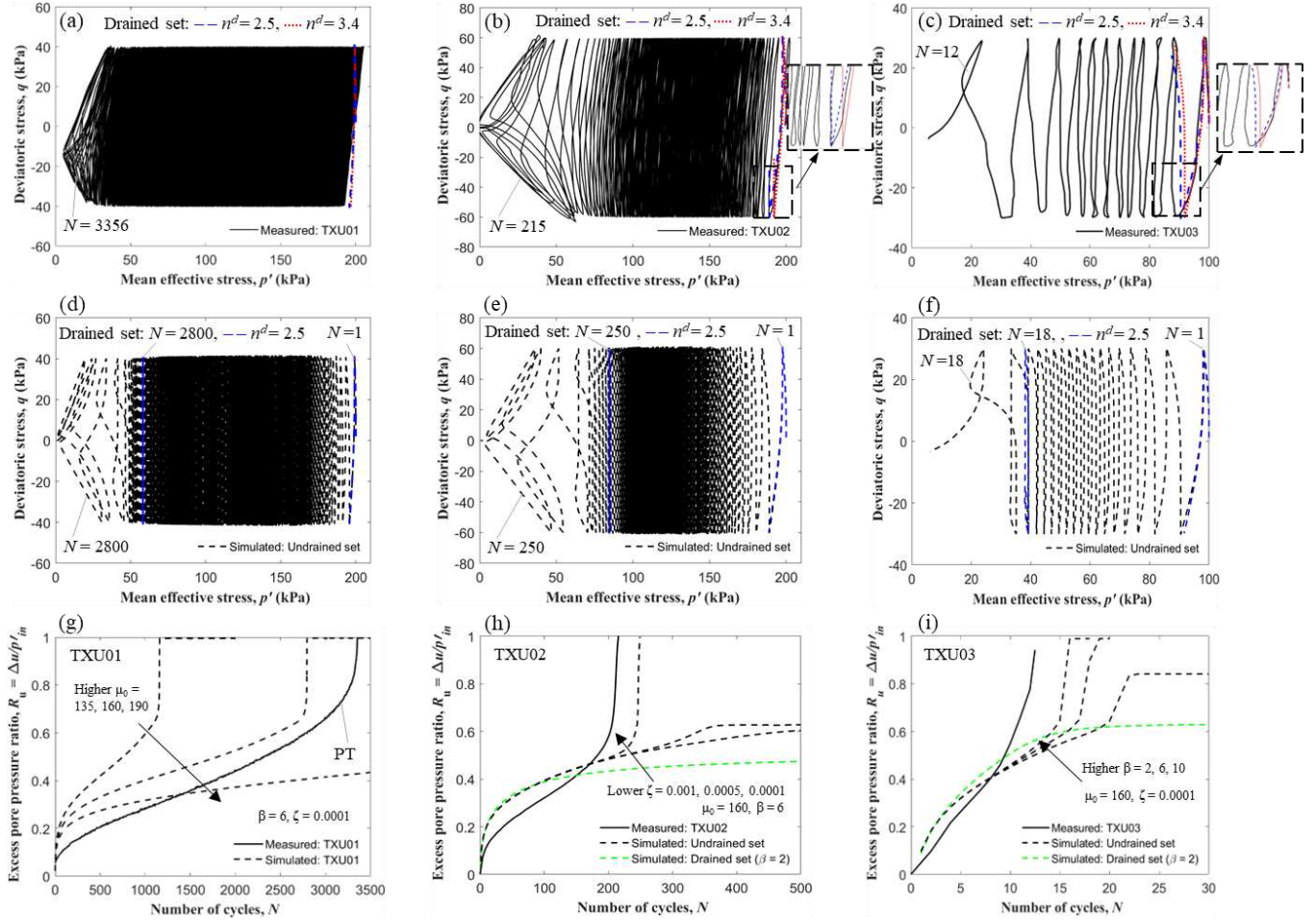


Figure 1. Undrained cyclic triaxial tests: (a-c) Measured against simulated response using the drained set; (d-f) Simulated response using the drained and undrained set; (g-h) recalibration of MS parameters using R_u paths

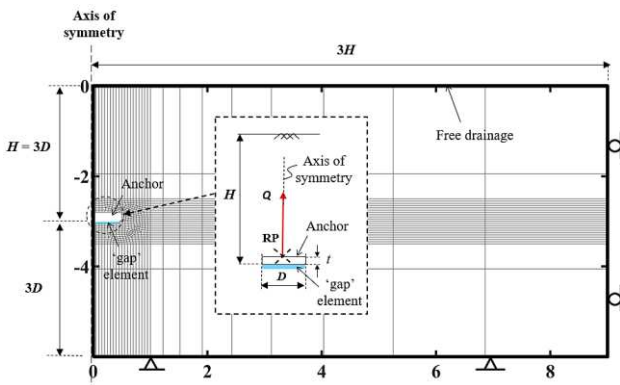


Figure 2. Geometry and boundary condition of FE model

4 PERFORMANCE OF THE NUMERICAL MODEL AGAINST CENTRIFUGE TESTS

The performance of the SANISAND-MS model was validated against identical prototype-scaled circular anchors in UWA silica sand of $I_D = 87.7\%$ (see

Table 4) at $N_g = 30g$. The model stainless-steel circular anchors, with a diameter (D) of 30 mm and thickness of 6 mm, were pre-embedded at an embedment ratio (H/D) of 3 in methocel-saturated fine silica sand. The Methocel F450 solution with dynamic viscosity (μ) of 169 mPa·s at 20 °C was used as pore fluid to reduce soil permeability (and thus c_v), enabling the desired partially drained response to be achieved in the experiments. The anchors were subjected to 5000 cycles of one-way vertical cyclic uplift load at a frequency of 0.5 Hz, with varying mean stress (q_m) and stress amplitude (q_a) as presented in Table 4.

Previous studies (e.g. Kurniadi et al. 2023, Roy et al. 2024) have shown that stress paths in a boundary value problem differ from those in element tests, thus adjustments to stiffness and dilatancy parameters (G_0 , h_0) in SANISAND-MS are needed to better match the initial mobilisation response for plate anchors. The adjusted values of $G_0 = 85$, $h_0 = 4.2$, $n^d = 2.8$ were needed for modelling the plate anchor responses under drained conditions (see Table 3), and the same

adjustment was used for the undrained set while modelling the plate anchor. Both sets of parameters (Table 3) were validated against Test C0.4-0.1M over 100 cycles (Figure 3).

The experiment measured uplift stress (q , minus anchor weight) with a normalised anchor displacement (δ/D) of 2% over 100 cycles (Figure 3). The simulations using undrained and drained parameters produced $\delta/D = 3.1\%$ and 0.4% respectively, which meant the undrained set simulated a softer response, whereas the drained set simulated a stiffer response.

Table 4. Centrifuge tests for numerical validation

Test ID*	Mean stress q_m (kPa)	Cyclic stress amplitude q_a (kPa)
C0.4-0.1M	107.6	26.9
C0.4-0.3M	107.6	80.7
C0.5-0.3M	134.5	80.7

* Each test was identified as CX_1-X_2M , where 'C' stands for cyclic load, 'X₁' and 'X₂' represent q_m and q_a respectively relative to the anchor monotonic uplift capacity (measured as 269 kPa), and 'M' stands for pore fluid, i.e. Methocel

Furthermore, a large δ/D was measured in the experiment between $N = 1$ and 10, possibly due to a non-uniform zone of soil around the anchor, as the sands rebound off the plate during sand raining. This feature was not captured in the simulations. Instead, if the accuracy of the simulation for C0.4-0.1M was evaluated by comparing the measured accumulated displacement between the 10th and 100th cycle (i.e. $(\delta_{max}/D)^{10th-100th} = 0.6\%$), then the simulated undrained and drained parameters would show a value of 2.8% and 0.2% respectively, suggesting that the simulations broadly capture the change in accumulated displacement.

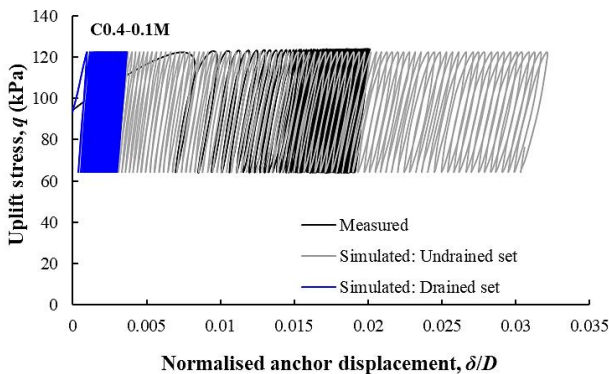


Figure 3. Comparison of measured and simulated accumulated displacement for Test C0.4-0.1M

In comparison to the undrained parameter set, the drained parameter set also produced a characteristic ratcheting behaviour and attained shakedown. Hence the drained parameter set has been chosen as the starting point for further investigation to match the

cyclic responses. To better predict the partially drained responses, the MS parameter β is now increased from 1 to 2 (Table 3), to promote stronger accumulated displacement and increased excess pore pressure (Δu).

Using the drained parameter set with $\beta = 2$, Figure 4 compares the simulated $(\delta_{max}/D)^{10th-100th}$ and normalised excess pore pressure ($\Delta u/\sigma'_{v0}$, with σ'_{v0} the initial vertical stress) against the experiments for the three partially drained tests (Table 5). The simulations can capture the experimental trend of increasing δ/D and $\Delta u/\sigma'_{v0}$ with the increase of Q_a and Q_m . The difference in $(\delta_{max}/D)^{10th-100th}$ between the experiments and simulations ranges from 19.1% to 43.9%. The simulation can also capture the magnitude of the maximum $\Delta u/\sigma'_{v0}$ (Table 5) but fail to capture the stabilization trend in $\Delta u/\sigma'_{v0}$ (Figure 4).

It is useful to examine the effect of adjusting β at element level. For the drained cyclic triaxial test reported in Roy et al. (2024), insignificant difference is observed in the strain accumulation simulated using $\beta = 1$ and 2 respectively (Figure 5). While for undrained cyclic triaxial tests, using $\beta = 2$ would result in stabilisation of Δu after several cycles (Figure 1h and i), which supports the measured Δu responses in the partially drained anchor tests (Figure 4).

Table 5. Comparison in $(\delta_{max}/D)^{10th-100th}$ and $\Delta u/\sigma'_{v0}$

Test ID	$(\delta_{max}/D)^{10th-100th}$		Max. $\Delta u/\sigma'_{v0}$	
	measured	simulated	measured	simulated
C0.4-0.1M	0.6%	0.4%	0.01	0.01
C0.4-0.3M	3.5%	2.9%	0.14	0.06
C0.5-0.3M	5.9%*	3.3%*	0.06	0.06

* terminated at 74 cycles

5 CONCLUSIONS

The performance of SANISAND-MS model has been assessed at element level and in a boundary value problem of circular plate anchors in dense sand under cyclic loading. Key findings from this study are:

- The model could capture the 'flow-type liquefaction' in loose sand but struggle to capture the 'cyclic mobility' in dense sand.
- The cyclic undrained triaxial tests showed higher contractancy, which required lowering n^d as compared to the drained responses.
- There is no single set of model parameters capable of capturing the full range of drainage conditions at both element level and plate anchor problem. The partially drained response of plate anchors could be better matched using the drained cyclic parameters, but with an adjusted β .
- The model reasonably predicted the accumulated displacement during partially drained cyclic loading across different cyclic mean stress and

amplitude from $N = 10$ to 100. At the same time, further investigations are needed to explore the

patterns in the simulated responses for $N = 1$ to 10.

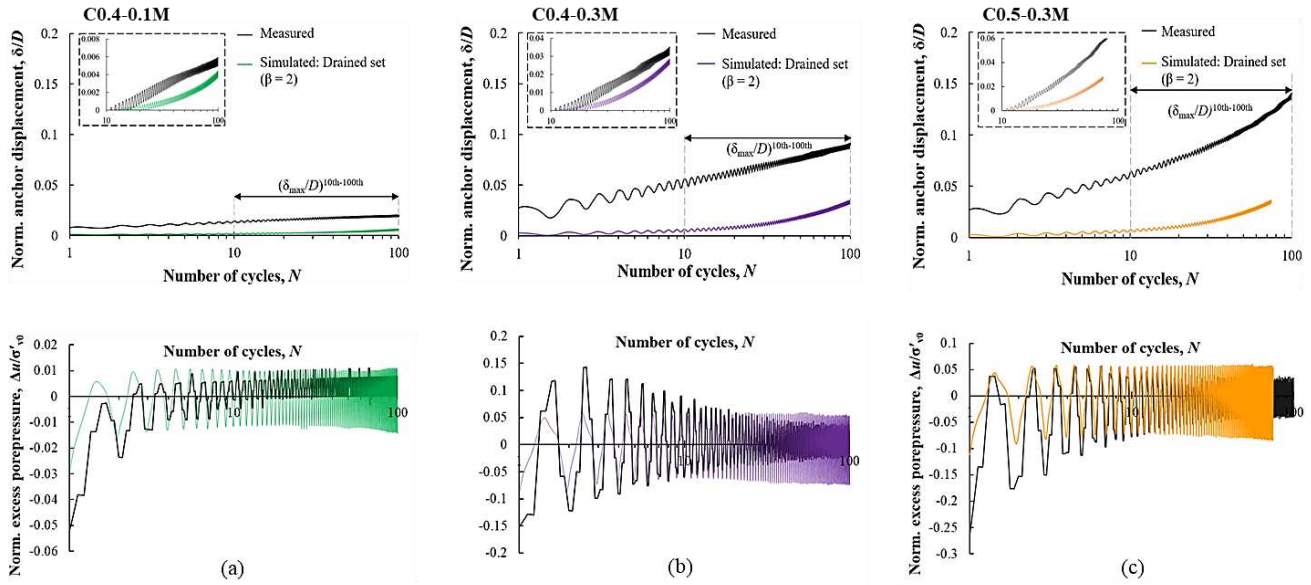


Figure 4. Comparison of accumulated displacement and normalised excess pore pressure between centrifuge test results and simulation (drained parameters with $\beta = 2$) for: (a) C0.4-0.1M; (b) C0.4-0.3M; and (c) C0.5-0.3M

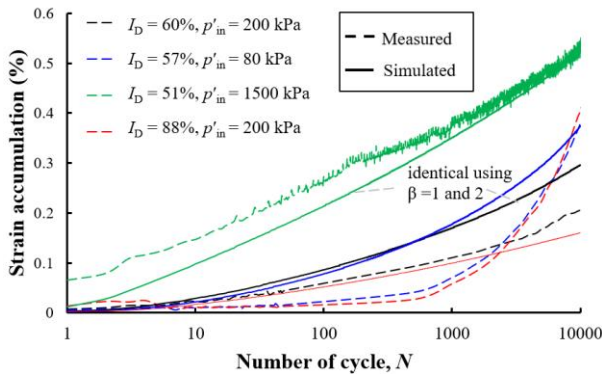


Figure 5. Effect of β on simulated drained triaxial cyclic test response using the drained set

AUTHOR CONTRIBUTION STATEMENT

R. Kurniadi: Writing – original draft, Investigation, Formal analysis, Validation, Visualization. **A. Roy:** Writing – review & editing, Visualization, Supervision, Conceptualization. **S.H. Chow:** Writing – review & editing, Visualization, Supervision, Funding acquisition. **M.J. Cassidy:** Writing – review & editing, Supervision.

ACKNOWLEDGEMENTS

The authors are grateful for the financial support provided by the Australia Government Research Training Program and by Australian Research Council Discovery Grant Scheme DP220101652.

REFERENCES

- Barrero, A., Taiebat, M., & Dafalias, Y. (2020, 02/25). Modeling cyclic shearing of sands in the semifluidized state. *International Journal for Numerical and Analytical Methods in Geomechanics*, 44, 371-388.
- Chow, S. H., Diambra, A., O'Loughlin, C. D., Gaudin, C., & Randolph, M. F. (2020). Consolidation effects on monotonic and cyclic capacity of plate anchors in sand. *Géotechnique*, 70(8), 720-731.
- Kurniadi, R., Roy, A., Chow, S. H., & Cassidy, M. J. (2023). Drained cyclic response of circular plate anchors in dense sand. *9th International SUT OSIG Conference*, 1590 - 1597.
- Liu, H. Y., Abell, J. A., Diambra, A., & Pisanò, F. (2019). Modelling the cyclic ratcheting of sands through memory-enhanced bounding surface plasticity. *Géotechnique*, 69(9), 783-800.
- Liu, H. Y., Zygounas, F., Diambra, A., & Pisanò, F. (2018). Enhanced plasticity modelling of high-cyclic ratcheting and pore pressure accumulation in sands. *9th European Conference on Numerical Methods in Geotechnical Engineering*.
- Maitra, S., White, D., Chatterjee, S., & Choudhury, D. (2019). Numerical modelling of seepage and tension beneath plate anchors. *Computers and Geotechnics*, 108, 131-142.
- Roy, A., Liu, H., Bienen, B., Chow, S. H., & Diambra, A. (2024). Suction bucket performance in sand under vertical cyclic loading: Numerical modelling using SANISAND-MS. *Computers and Geotechnics*, 173, 106497.

INTERNATIONAL SOCIETY FOR SOIL MECHANICS AND GEOTECHNICAL ENGINEERING



This paper was downloaded from the Online Library of the International Society for Soil Mechanics and Geotechnical Engineering (ISSMGE). The library is available here:

<https://www.issmge.org/publications/online-library>

This is an open-access database that archives thousands of papers published under the Auspices of the ISSMGE and maintained by the Innovation and Development Committee of ISSMGE.

The paper was published in the proceedings of the 5th International Symposium on Frontiers in Offshore Geotechnics (ISFOG2025) and was edited by Christelle Abadie, Zheng Li, Matthieu Blanc and Luc Thorel. The conference was held from June 9th to June 13th 2025 in Nantes, France.